Available online at www.sciencedirect.com
ScienceDirect
Tetrahedron
Tetrahedron 63 (2007) 12396–12404

Subphthalocyanine fused dimers–C_{60} dyads: synthesis, characterization, and theoretical study

Rodrigo S. Iglesias,[a] Christian G. Claessens,[a] G. M. Aminur Rahman,[b] M. Angeles Herranz,[c] Dirk M. Guldi[b,*] and Tomas Torres[a,*]

[a]*Departamento de Química Orgánica, Universidad Autónoma de Madrid, 28049 Madrid, Spain*
[b]*Friedrich-Alexander-Universität Erlangen-Nürnberg, Egerlandstrasse 3, Department of Chemistry and Pharmacy, Interdisciplinary Center for Molecular Materials (ICMM), 91058 Erlangen, Germany*
[c]*Departamento de Química Orgánica, Facultad de Química, Universidad Complutense de Madrid, E-28040 Madrid, Spain*

Received 4 July 2007; revised 17 September 2007; accepted 20 September 2007
Available online 26 September 2007

Abstract—A donor–acceptor covalently linked dyad consisting of a subphthalocyanine fused dimer unit doubly-connected to a [60]fullerene has been prepared through double cycloaddition of the fused dimer, previously functionalized with aldehyde groups in the axial positions, to the fullerene (1,3-dipolar cycloaddition of azomethine ylides). The compound, isolated in several fractions, has been characterized and studied employing photophysical and electrochemical techniques. Molecular modeling of the distinct possible isomers was carried out using semi-empirical methods.

1. Introduction

The investigation of donor–acceptor systems based on [60]fullerene was found to be utmost importance in the field of materials chemistry.[1] The interest in such ensembles relies on the excellent acceptor properties of C_{60}, capable of receiving up to six electrons.[2] When linked to a donor counterpart, which usually serves as a light-harvesting unit, these fullerene-based systems undergo a cascade of photoinduced processes, which have found applications in photovoltaic, switching, or sensor devices.[3]

Among C_{60}-based donor–acceptor ensembles, those including porphyrins and phthalocyanines as donor units[4] are of special relevance since these chromophores absorb strongly in the visible region, and this absorption may be fine-tuned through chemical modifications of the macrocycle.

Subphthalocyanines (SubPcs, **4**, Fig. 1)—lower homologs of phthalocyanines made of three isoindole units *N*-fused around a boron atom with outstanding NLO properties[5]—have been employed also successfully in the preparation of donor–acceptor systems[6] by means of the chemically accessible axial position of this macrocycle.

Moreover, the subphthalocyanine macrocycle, as a non-planar aromatic molecule, is an ideal supramolecular probe for studying non-covalent interactions between non-planar π-surfaces.[7] Thus, both concave–concave and concave–convex[8] interactions between SubPc and C_{60} were probed by covalent linking between the two species or supramolecular inclusion within a self-assembled subphthalocyanine capsule.[8]

Recently, an improved synthetic method[9] allowed the efficient synthesis of subphthalocyanine fused dimers[10] and trimers, and separation (in the case of the dimers) of their *syn* and *anti* topoisomers (Fig. 1, compounds **2a** and **2b**). SubPc dimers, while bearing two axial positions, allow the interesting possibility (for the *syn* topoisomer) of a double connection to a single C_{60} fragment.[11] This double connection through the convex face of the macrocycle, forces the docking of the C_{60} unit in a relatively fixed position, suitable for through-space interactions between the donor (SubPc dimer) and acceptor units (C_{60}).

Herein, a detailed account of the synthesis and the photophysical and electrochemical characterizations of a SubPc dimer–C_{60} dyad (**1**, Fig. 1) will be given. A thorough theoretical study at semiempirical level will also provide an exhaustive view of the possible constitutional isomers and their likely distribution.

2. Results and discussion

Dyad **1** was prepared following a procedure developed in our laboratory,[6] in which the functionalization of C_{60} is achieved

Keywords: Subphthalocyanine; [60]Fullerene bisadducts; Photophysics; Electrochemistry.
* Corresponding authors. Tel.: +34 914974151; fax: +34 914973966; e-mail: tomas.torres@uam.es

0040–4020/$ - see front matter © 2007 Elsevier Ltd. All rights reserved.
doi:10.1016/j.tet.2007.09.051

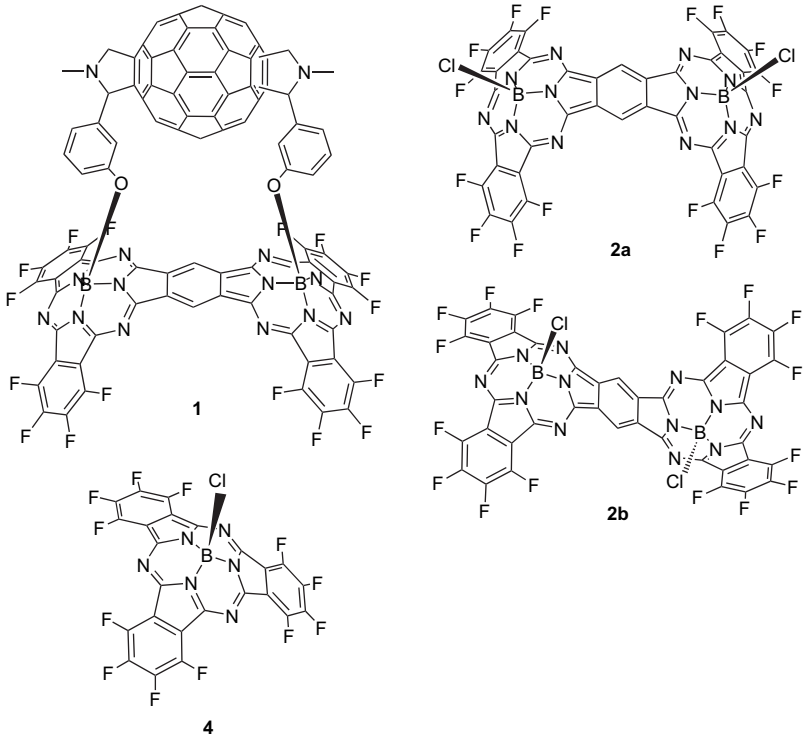

Figure 1. Subphthalocyanine fused dimer–C_{60} dyad (**1**), subphthalocyanine fused dimers (**2a** and **2b**), and 'monomeric' subphthalocyanine (**4**).

by 1,3-cycloaddition of an azomethine ylide (the so-called Prato reaction) (Fig. 2).

syn-Dialdehyde **3a** was prepared in 3% yield in a two-step one-pot reaction by statistical condensation of 1,2,4,5-tetracyanobenzene with an excess of tetrafluorophthalonitrile (1–10 M) in the presence of BCl_3 in *p*-xylene at 140 °C for 2–3 h[10] followed by axial chlorine substitution with 3-hydroxybenzaldehyde in toluene at reflux for 20 h.[9] Surprisingly, the *anti* isomer **3b** could not be isolated from the same reaction and even more surprisingly only decomposition products could be observed when the axial substitution was carried out from pure dichloro *anti* isomer **2b**.

syn-Dialdehyde **3a** was then reacted with *N*-methylglycine and C_{60} in toluene at reflux giving rise to the C_{60}–SubPc dimer ensemble **1** in 14% yield.

The isomeric mixture **1** was unambiguously characterized by ^{1}H NMR spectroscopy, MALDI-TOF mass spectrometry, and elemental analysis. However, it was not possible to separate any of the multiple isomers in the purification procedure (column chromatography on silica gel). This mixture of isomers gave rise to a very complex ^{1}H NMR spectrum that could only be interpreted by considering the expected chemical shifts' ranges for known protons and their respective integration.

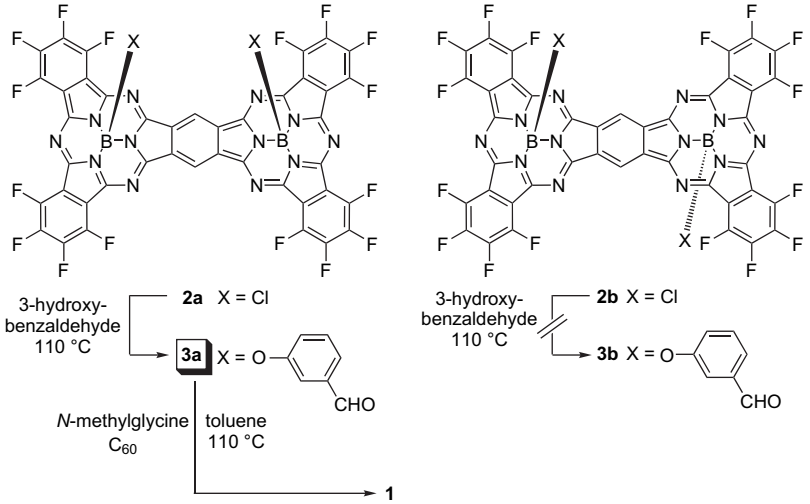

Figure 2. Synthesis of SubPc dimer–C_{60} **1**.

UV–vis spectra of dyad **1** and its precursor **2a** are very similar, although a small increase in the absorption around 490 nm is observed with the incorporation of the C_{60} subunit. According to previous studies,[12] this change is consistent with the presence of a *trans* substitution pattern (see Section 2.3).

2.1. Photophysics

A series of photophysical experiments were performed on dyad **1** and on a reference dichloro *syn* dimer **2a**, in order to determine the dynamics of the different deactivation routes following photoexcitation. [60]Fullerene measurements were also carried out as reference.

The emission spectra of the SubPc dimers are clearly not a mirror image of the absorption band (Fig. 3), which is also a characteristic of asymmetric SubPcs. The blue-end peaks are not visible in the emission profile as they arise from higher energy transitions due to the orbital split-up in the SubPc dimers and low-symmetry subphthalocyanines, while the emission takes place only from the lowest excited state.

The double linking of a C_{60} molecule to **2a** leads in the ground state to minute perturbations of the π-electronic structure of the SubPc dimer core. When photoexciting **1**, on the other hand, the fluorescence quantum yields decrease strongly. In toluene, THF, and benzonitrile quantum yields are as low as 0.02±0.01, which corresponds to a 12-fold quenching. Despite the significant quenching, the fluorescence spectra of **1** and **2a** are strict superimpositions, that is, no quenching products can be assigned based on these experiments. The C_{60} reference fluoresces in the same spectral region with quantum yields of ca. 10^{-4}.

Fluorescence decay measurements shed light onto the SubPc dimer deactivation route (in the dyad **1** and reference **2a**) after photoexcitation (Fig. 4). The fluorescence-time profiles for **1** are best fitted by bi-exponential expressions, while **2a** shows best fits with a mono-exponential expression. In all solvents, a short-lived (0.27±0.02 ns) and a long-lived (1.2±0.05 ns) components for the bi-exponential were found. The short lifetime contribution reflects the prompt deactivation of the SubPc dimer singlet excited state, while the long-lived contribution resembles that of the C_{60} reference.

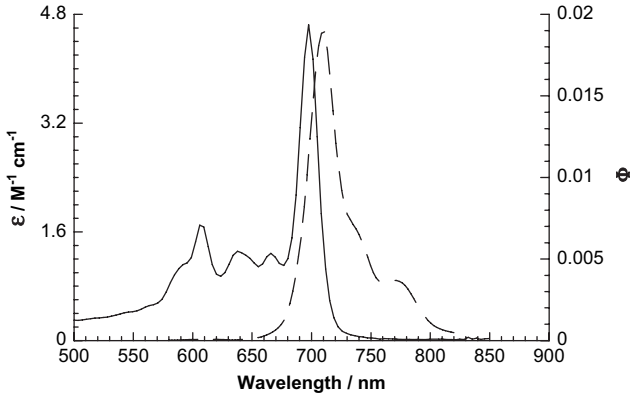

Figure 3. Absorption and emission spectrum of **1** in toluene—excitation wavelength is 550 nm.

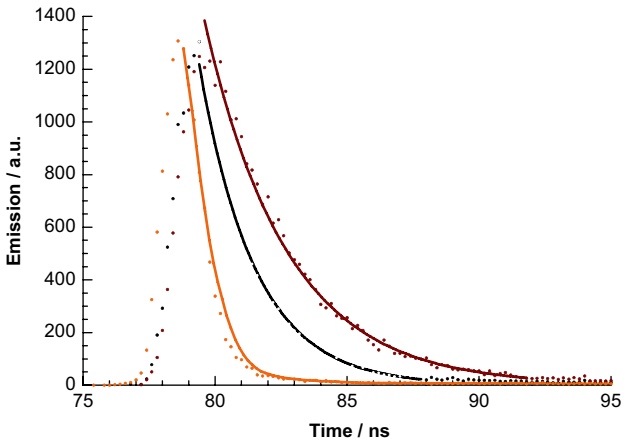

Figure 4. Time resolved fluorescence decay of **2a** (red line), **1** (black line), and laser scatterer (orange line) in room temperature solutions (5×10^{-6} M)—excitation wavelength is 337 nm and monitoring wavelength is 710 nm.

This allows to postulate that the former contribution is due to a transference of singlet excited state energy from the SubPc dimer to C_{60}, which are nearly isoenergetic (1.77 eV for the SubPc dimers and 1.76 eV for the fullerene). Once the singlet excited state energy is funneled to the C_{60} core, intersystem crossing populates the triplet manifold.

Femtosecond laser pulses were employed to visualize the different photoproducts. Typical differential absorptions, recorded with several time delays—0.4 ps—following photoexcitation of **2a**, are shown in Figure 5a. In particular, a strong transient bleach is seen at the Q-band maxima (700 nm). The underlying singlet excited state intersystem crosses slowly to the triplet manifold. Photoexciting compound **1** within the same time frame led to the similar absorption changes. This confirms the formation of the SubPc dimer singlet excited state.

From nanosecond differential absorption experiments it was possible to identify the triplet states. Figure 5b shows that the characteristic C_{60} triplet–triplet strong transition at 700 nm is not visible. Instead, the only detectable photoproduct is that of the SubPc dimer triplet excited state with a 1080 nm peak possessing a long lifetime (107 μs) and a high triplet quantum yield (95% of that seen for **2a**).

In summary, these experiments establish a cascade of energy transfer events for the SubPc dimer–C_{60} dyads, transducing the excitation energy back and forth between the two moieties, which are illustrated in Figure 6. It should be mentioned that analog dodecafluoro-substituted SubPc–C_{60} dyads undergo similar deactivation routes of the excited singlet state, even if the excited singlet state of the subphthalocyanine–C_{60} possess a much higher energy (~2 eV).[6b]

2.2. Electrochemical measurements

The redox behavior of dyad **1**, the SubPc dimers **2a**, **2b**, and **3a**, and the reference SubPc **4** was investigated by cyclic voltammetry (CV) and Osteryoung square-wave voltammetry (OSWV) in THF solutions under an argon atmosphere. The redox potentials obtained (vs Fc/Fc^{+}) are summarized

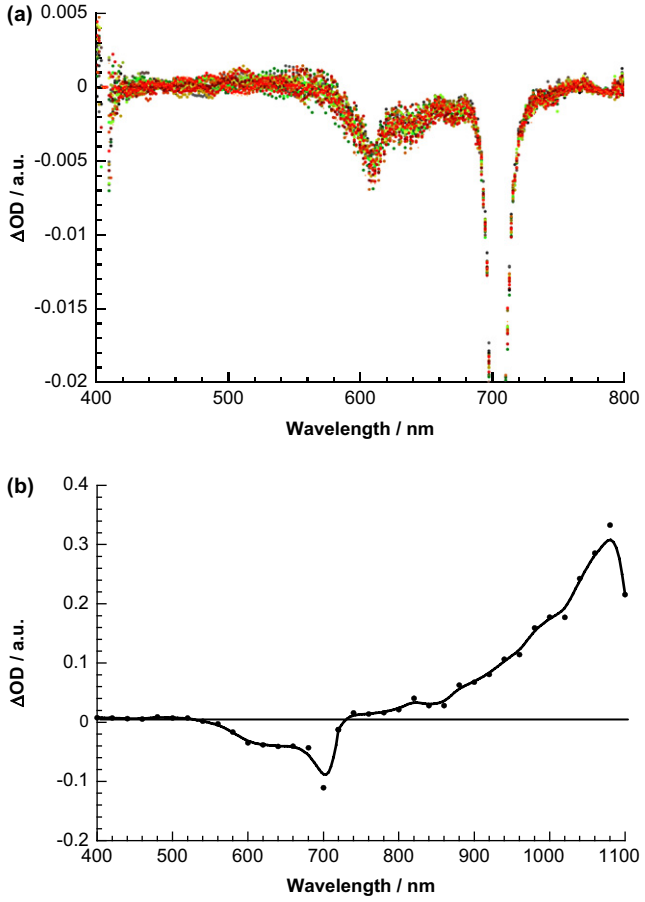

Figure 5. (a) Differential absorption spectrum (visible) was obtained upon femtosecond flash photolysis (391 nm) of ~1.0×10^{-5} M solutions of **2a** in nitrogen saturated toluene with a several time delay between 0 and 4 ps at room temperature. The spectrum corresponds to the changes that are associated with the formation of the SubPc dimer singlet excited state. (b) Differential absorption spectrum (visible and near-IR) was obtained upon nanosecond flash photolysis (532 nm) of ~5.0×10^{-6} M solutions of **1** in nitrogen saturated toluene with a time delay of 50 ns at room temperature. The spectrum corresponds to the changes that are associated with the formation of the SubPc triplet singlet excited state.

in Table 1 and the CVs are shown in Figure 7. As expected, SubPc **4** presents the characteristic several reduction waves of SubPcs, with a reversible first reductive process that involves one electron.[5a] An irreversible oxidation is observed for this SubPc at +1001 mV, being this SubPc, endowed with strong electron-withdrawing fluoro substituents, one of the hardest to oxidize reported so far.[5a]

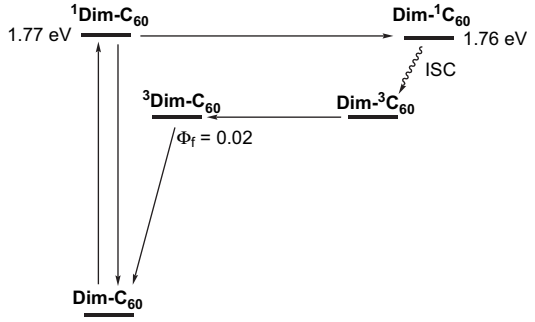

Figure 6. Photophysical processes occurring upon SubPc dimer excitation of dyad **1** in toluene.

The optical properties of dimers **2a**, **2b**, and **2c** anticipated a strong π-extended electronic interaction between both subphthalocyanine structures that was confirmed by electrochemical means. In Figure 7, it is clearly observed how the SubPc subunits do not behave independently, and the extraction/addition of one electron from/to one of the SubPc subunits strongly affects the redox processes on the other ring. These observations clearly confirm that the SubPc dimers are fully conjugated.[10]

SubPc dimers **2a**, **2b**, and **2c** exhibit a first oxidation process 100–150 mV negatively shifted when compared to those of the corresponding SubPc **4**. The second oxidation process, which takes place in the other SubPc subunit, appears up to 190 mV positively shifted when compared with the first one. In the cathodic scan, the three SubPc dimers studied exhibit several reduction peaks, with the first two always being reversible and corresponding to the first redox processes on each one of the SubPc subunits. At more negative potentials several processes were observed, being the reversibility of them slightly influenced by the substitution on the macrocycle. The strong coupling existing between both SubPc subunits is also evidenced by the approximately 100 mV positive shift that the first reduction potentials experiment when compare with SubPc **4**.The second reduction processes of these dimers, which take place in the other SubPc subunit, appear up to 300 mV negatively shifted when compared with the first ones.

It is generally accepted that the increase in the number of addends on C_{60} produces structural modifications that result in compounds progressively more difficult to reduce.[13] In this sense, fullerene bisadducts reduction potentials are around 200 mV negatively shifted with respect to C_{60}.[14] For comparison purposes the electrochemistry of a mixture of fullerene bisadducts endowed with methyl fulleropyrrolidines was investigated, in our experimental conditions three quasi-reversible reduction waves were obtained for this mixture of compounds at −1138, −1672, and −2397 mV.

Dyad **1** retains the irreversible oxidation processes observed for the corresponding SubPc dimer **3a**.These oxidative processes appear to be 40 mV negatively shifted in the dyad. On the reduction scan, to assign the electrochemical processes to one electroactive unit or to the other is complicated in such a multielectronic system. The first reversible wave is assigned to the first reduction in one of the SubPc subunits of the dimer, this first reduction peak appears 55 mV negatively shifted when compared with SubPc dimer **3a**. The second and third reductions of this dyad are two-electron processes, which involve the second reduction of the SubPc dimer and the first reduction on the C_{60} core. The electrochemical data show that the redox potentials of the SubPc moiety in dyad **1** change to some extend when compare to that of the model compound **3a**, which might be an indication of an electronic interaction between both electroactive units (C_{60} and the SubPc dimer) in the ground state.

2.3. Molecular modeling

Dyad **1** was also studied employing quantum chemical calculations at semiempirical level (AM1 parameterization).[15] From the eight possible isomers resulting from bisaddition

Table 1. Redox potentials obtained from cyclic voltammetry for the reference subphthalocyanine **4**, subphthalocyanine dimers **2a**, **2b**, and **3a**, and fused dimer–C_{60} dyad **1** (THF, in mV vs Fc/Fc^{+})

Compound	E^{1}_{ox} [a]	E^{2}_{ox} [a]	$E^{1}_{1/2,\ red}$	$E^{2}_{1/2,\ red}$	$E^{3}_{1/2,\ red}$	$E^{4}_{1/2,\ red}$	E^{5}_{red} [b]	E^{6}_{red} [b]
1	+800	+955	−930	−1213	−1751	—	−2199	−2409
2a	+870	+1060	−820	−1129	−1551[b]	−1773[b]	−2020	−2384
2b	+907	+1041	−836	−1130	−1685[b]	−1918[b]	—	−2690
3a	+841	+998	−875	−1171	−1544	−1840	−2089	—
4	+1001	—	−923	—	−1614[b]	—	−2039	−2495

[a] Since these oxidative processes are irreversible, only anodic peak potentials are reported.
[b] Since these reductive processes are irreversible, only cathodic peak potentials are given.

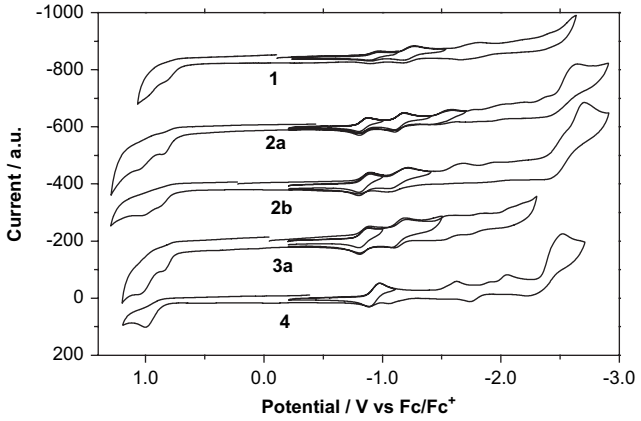

Figure 7. Cyclic voltammograms of the subphthalocyanine fused dimer–C_{60} dyad **1**, the reference subphthalocyanine **4**, and the bicyclic subphthalocyanine dimers **2a**, **2b**, and **3a**.

to C_{60} (Fig. 8),[16] six (*trans*-**1**, *trans*-**2**, *trans*-**3**, *trans*-**4**, *e*, and *cis*-**3**) were fully optimized (with 0.1 gradient rms cut-off). Highly strained *cis*-**1** and *cis*-**2** isomers were not considered. For comparison, a hypothetic structure where a dimer with chlorines in the axial position and a *trans*-**1** bisfulleropyrrolidine are non-covalently bonded was optimized.

Each bisadduct regioisomer is in fact a mixture of two different isomers, depending on which side of the pyrrolidine ring the rest of the structure is connected as shown in Figure 9a. Finally, the chiral carbon atom on the pyrrolidine gives rise to a diastereomeric mixture for each of the above-mentioned isomers (Fig. 9b).

All of these structures were optimized semiempirically, except for the cases where structural restrictions forbid the connection between the C_{60} and the dimer moieties. Furthermore, two conformations were optimized for each isomeric form, the first one with both phenyl rings oriented in the same direction, and the other with the rings in opposite directions as illustrated in Figure 10.

Table 2 presents results of heat of formation for each optimized geometry, along with some structural parameters. According to these calculations, the most thermodynamically stable regioisomers (in average) are those from the *trans*-**3** series, while those belonging to the *cis*-**3** addition pattern, as expected, are the less stable ones.

The heat of formation for those C_{60}–subphthalocyanine dimer adducts was found to be in good correlation with the distance between the C_{60} moiety and the dimer subunit as shown in Figure 11.[17]

trans-**1** structures are not, as could be expected, among the most stable ones. The calculated structures for this isomer display a relatively large energy of formation associated to a shorter distance between the C_{60} and dimer subunits (3.40 Å) than the 'equilibrium' distance calculated in the non-covalent dimer/bisfulleropyrrolidine structure (3.90 Å, Fig. 12).[18]

The shorter is the distance between the pyrrolidine units (*cis*-**3** and *e*), the larger is the distance between the two moieties, reaching up to 7.3 Å. In these cases, instability is caused by the highly strained geometry, which is clearly illustrated by the significant deformation observed in the dimer subunit.

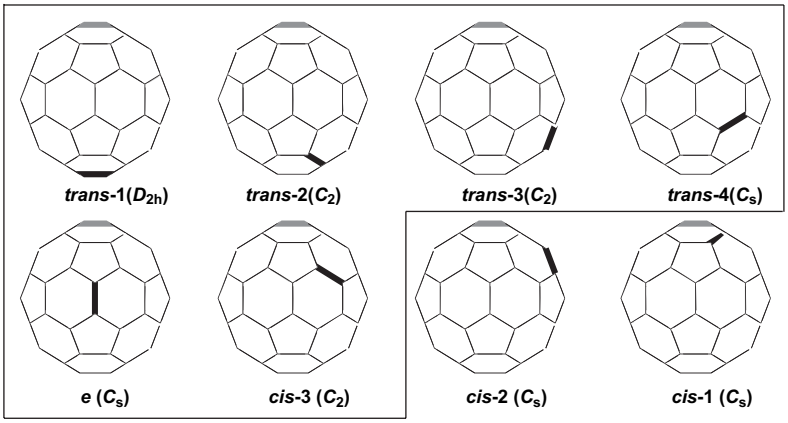

Figure 8. Eight possible isomers of [C_{60}]fullerene from bisaddition to [6,6] bonds.

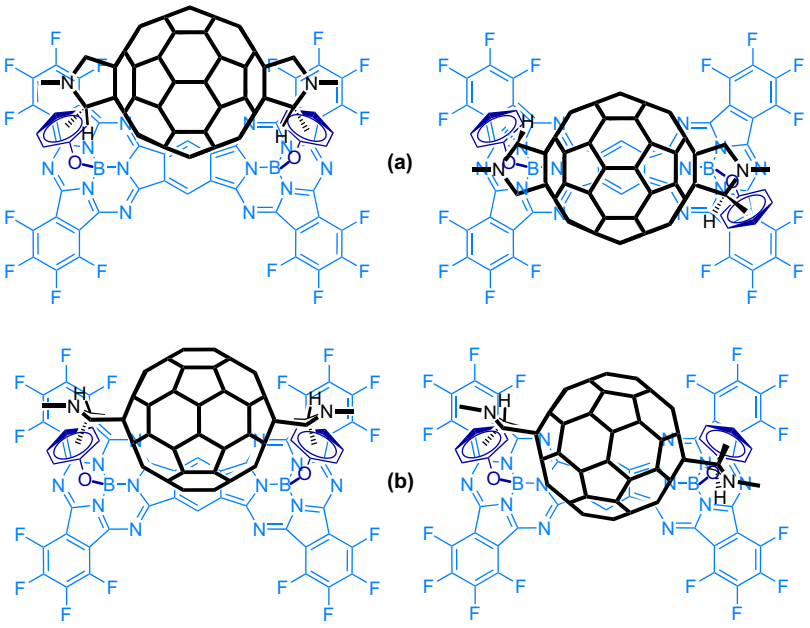

Figure 9. Example of the possible isomers (a) and diastereomers (b) of compound **1** for one of the C_{60} bisadducts (*trans*-**1**).

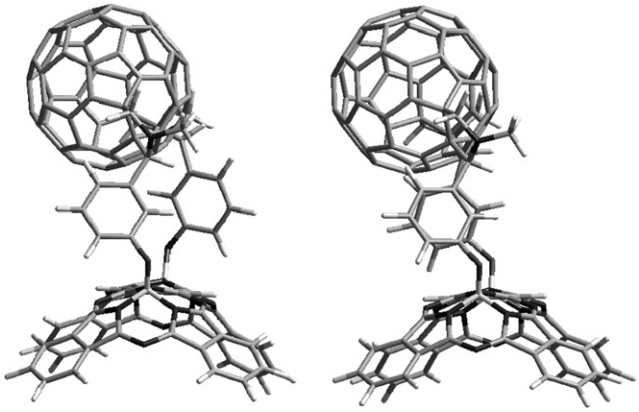

Figure 10. Two possible orientations of the phenyl rings linking the dimer to the fullerene unit.

The deviation of the C_{60} subunit from the C_{2v} axis of the dimer was also measured for all the calculated structures. This parameter varies from nearly zero (in a *trans*-**1** structure) to 5.7 Å (*cis*-**3**). No significant correlation is observed for this parameter that shows large deviations even among the same regioisomer.

3. Concluding remarks

A novel subphthalocyanine fused dimer–C_{60} (**1**) covalent ensemble has been successfully prepared and characterized. Photophysical studies reveal that this dyad undergoes a series of energy transfer events similar to those observed in SubPc–C_{60} analogs. After photoexcitation of the donor unit (dimer), a singlet–singlet energy transfer to the acceptor fullerene, which decays by intersystem crossing to the C_{60} triplet state, ends with the energy back-transfer to the dimer triplet state. In contrast with SubPc–C_{60} dyads, the singlet–singlet transfer in the dimer–C_{60} dyad occurs between nearly isoenergetic states, as the dimer S_1 state lies at a significantly lower energy (1.77 eV) than that of SubPc (2.1 eV), thus being very close to the S_1 state of C_{60}-fullerene (1.76 eV). Electrochemical measurements confirmed the strong electronic coupling existing between the SubPc subunits of dimers **2a**, **2b**, and **3a**, and showed small shifts in the redox potentials of SubPc and C_{60} units in dyad **1** when compared with reference systems. These differences might be due to some ground state interactions between both electroactive units. Although no separation of the C_{60} double addition regioisomers was achieved, simple molecular modeling of six of the eight possible bisadducts indicates that *trans*-**3** regioisomers are the most stable in average. The distance between the dimer and C_{60} subunits increases going from regioisomers with farthest separation of the pyrrolidine rings (*trans*-**1**) to the closest one (*cis*-**3**), and a reasonable correlation was found between this distance and the thermodynamic stability of the structure.

4. Experimental

4.1. General remarks

UV–vis spectra were recorded with a Hewlett–Packard 8453 instrument. IR spectra were recorded on a Bruker Vector 22 spectrophotometer. HRMS spectra were determined on a VG AutoSpec instrument. MALDI-TOF MS were recorded with a Bruker Reflex III spectrometer. NMR spectra were recorded with a BRUKER AC-300 instrument and a BRUKER DRX-500 instrument. NMR data: chemical shifts are given in parts per million, coupling constants are given in hertz. Column chromatographies were carried out on silica gel Merck-60 (230–400 mesh, 60 Å), and TLC on aluminum sheets precoated with silica gel 60 F_{254} (E. Merck). Chemicals were purchased from Aldrich Chemical Co. and TCI and used as received without further purification.

Table 2. Calculated properties and structural parameters of several isomers of compound **1**

Structure		ΔH_f[a] (kcal mol^{-1})	d (C_{60}–dimer)[b] (Å)	d (B–B)[c] (Å)	Structure		ΔH_f (kcal mol^{-1})	d (C_{60}–dimer) (Å)	d (B–B) (Å)
trans-**1**	**A1**[d]	1416.00	3.19	9.78	*trans*-**4**	**A1**	1397.35	6.77	9.65
	A2	1404.44	3.30	9.79		**A2**	1393.42	6.56	9.64
	B1	1394.60	3.44	9.77		**B1**	1389.85	5.65	9.75
	B2	1395.55	3.25	9.78		**B2**	1389.88	6.00	9.75
	C1	1388.71	3.67	9.80		**C1**	1385.22	5.74	9.75
	C2	1390.38	3.53	9.80		**C2**	1396.76	6.04	9.74
	Avg.	*1398.28*	*3.40*	*9.79*		**D1**	1390.11	5.06	9.76
trans-**2**	**A1**	1395.51	3.97	9.78		**D2**	1391.93	4.33	9.78
	A2	1385.65	4.31	9.78		Avg.	*1391.81*	*5.77*	*9.73*
	B1	1387.77	4.22	9.78	*e*	**A1**	1398.00	7.16	9.59
	B2	1382.94	4.21	9.79		**A2**	1401.81	7.19	9.42
	C1	1400.72	3.64	9.79		**B1**	1409.34	7.28	9.26
	C2	1409.51	3.35	9.81		**B2**	1398.18	6.83	9.52
	Avg.	*1393.68*	*3.95*	*9.79*		Avg.	*1401.83*	*7.12*	*9.45*
trans-**3**	**A1**	1384.08	5.35	9.74	*cis*-**3**	**A1**	1408.81	7.33	9.32
	A2	1388.30	5.67	9.77		**A2**	1404.06	6.96	9.28
	B1	1391.32	5.83	9.77		**B1**	1408.30	6.58	9.28
	B2	1401.06	5.64	9.76		**B2**	1412.75	6.63	9.48
	C1	1386.01	4.26	9.79		Avg.	*1408.48*	*6.88*	*9.34*
	C2	1381.15	4.30	9.79	Non-bonded C_{60}+dimer		*1321.96*	*3.92*	*9.71*
	D1	1387.72	4.08	9.77					
	D2	1383.80	4.80	9.78					
	Avg.	*1387.93*	*4.99*	*9.77*					

[a] Heat of formation.
[b] Shortest distance between the C_{60} and the dimer (central ring) subunits.
[c] Distance between the boron atoms of the dimer.
[d] Letters represent different isomers and diastereomers, numbers represent different conformations (see below for more information).

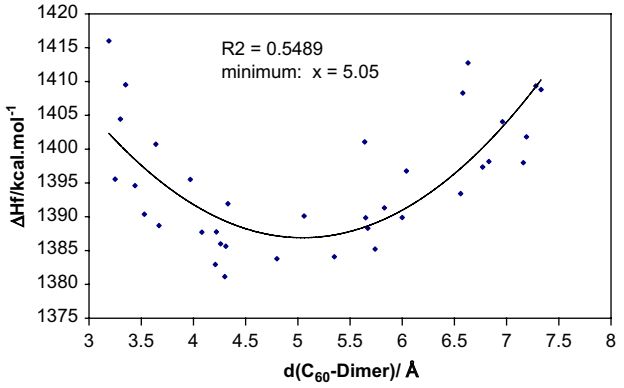

Figure 11. Correlation between the calculated heat of formation (ΔH_f) versus the shortest distance between C_{60} and dimer moieties for all the optimized structures.

4.1.1. *syn*-(Dichloro)(hexadecafluoro)-subphthalocyanine fused dimer 2a. BCl_3 (10.1 mL of a 1 M solution in *p*-xylene, 10.1 mmol) was added to a solid mixture of tetrafluorophthalonitrile (561 mg, 2.81 mmol) and 1,2,4,5-benzenetetracarbonitrile (50 mg, 0.28 mmol) in a 50 mL flask under argon atmosphere. The reaction mixture was refluxed for 2 h and after cooling down to room temperature, was flushed with argon. The resulting dark purple slurry was then evaporated under vacuum and subjected to various column chromatographies on silica gel using acetone/hexane (1:0 to 1:4, v/v) as eluent. Compound **2a** was isolated as a reddish blue powder (33 mg, 11%) (Found: C, 47.61; H, 0.31; N, 15.51. $C_{42}H_2B_2Cl_2F_{16}N_{12}$ requires: C, 47.10; H, 0.19; N, 15.69%.); ν_{max} (KBr)/cm^{-1} 1535, 1481, 1400, 1273, 1219, 1165, 1111, 1070, 1016, 966, 856, 795, 708, 658, 586; δ_H (300 MHz; $CDCl_3$; Me_4Si) 10.46 (2H, s); λ_{max} ($CHCl_3$)/nm 693 (log ε 4.9), 661 (4.4), 635 (4.4), 604 (4.5), 592 (sh), 441 (3.7), 319 (4.5), 278 (4.4); *m*/*z* (HR-LSIMS) 1069.9825 (M^+). $C_{42}H_2B_2Cl_2F_{16}N_{12}$ requires 1069.9833.

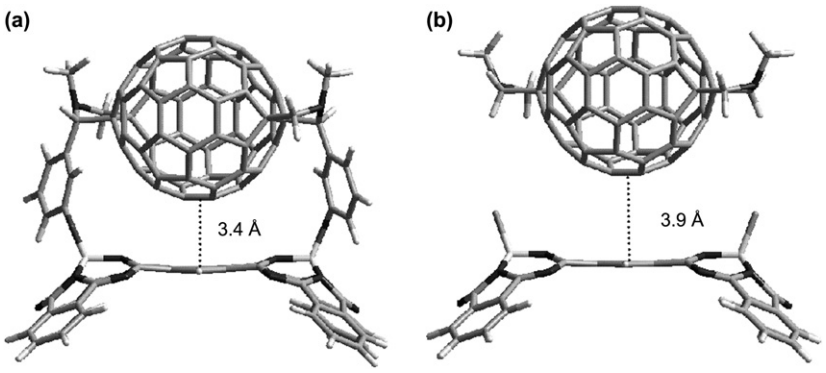

Figure 12. Dimer–C_{60} distances (average) in *trans*-**1** bisadducts (a) and in the non-covalently linked structure (b).

4.1.2. *anti*-(Dichloro)(hexadecafluoro)-subphthalocyanine fused dimer 2b. Isolated in the same conditions used for **2a**, as a reddish blue powder (27 mg, 9%) (Found: C, 47.56; H, 0.26; N, 15.25. $C_{42}H_2B_2Cl_2F_{16}N_{12}$ requires: C, 47.10; H, 0.19; N, 15.69%.); ν_{max} (KBr)/cm^{-1} 1539, 1487, 1400, 1285, 1225, 1165, 1115, 1067, 1020, 962, 858, 789, 638, 592, 557; δ_H (300 MHz; $CDCl_3$; Me_4Si) 10.48 (2H, s); λ_{max} ($CHCl_3$)/nm 692 (log ε 4.9), 662 (4.4), 636 (4.4), 605 (4.5), 592 (sh), 441 (3.9), 320 (4.5), 278 (4.4); *m/z* (HR-LSIMS) 1069.9845 (M^+). $C_{42}H_2B_2Cl_2F_{16}N_{12}$ requires 1069.9833.

4.1.3. *syn*-[Bis(3-hydroxybenzaldehyde)(hexadecafluoro)]-subphthalocyanine fused dimer 3a. The same reaction conditions employed to prepare compounds **2a** and **2b** were used in all three methods described below. Reactant amounts are specified in each case.

Method a: BCl_3 (1 M solution in *p*-xylene, 7.5 mL, 7.5 mmol), tetrafluorophthalonitrile (1.17 g, 5.8 mmol), and 1,2,4,5-benzenetetracarbonitrile (104 mg, 0.58 mmol). After solvent removal, 5 g (40 mmol) of 3-hydroxybenzaldehyde were added. The mixture was heated to 120 °C for 6 h. The crude was washed with methanol/water 1:1 to remove excess of the aldehyde and then filtered. The solid obtained was subjected to column chromatography on silica gel using hexane/dichloromethane/acetone (4:2:1, v/v) as eluent. Compound **3a**, 21 mg (3%), was obtained as a reddish blue powder (Found: C, 54.55; H, 0.71; N, 14.01. $C_{56}H_{12}B_2F_{16}N_{12}O_4$ requires: C, 54.14; H, 0.97; N, 13.53%.); ν_{max} (KBr)/cm^{-1} 2921, 1598, 1534, 1481, 1263, 1155, 1083; δ_H (300 MHz; $CDCl_3$; Me_4Si) 10.39 (2H, s), 9.71 (2H, s, CHO), 7.29 (2H, d, J_o 7.9), 7.07 (2H, t, J_o 7.8), 6.06 (2H, s), 5.72 (dd, J_o 7.8, J_m 1.4); λ_{max} ($CHCl_3$)/nm 691 (log ε 5.0), 660 (4.4), 633 (4.5), 603 (4.5), 590 (sh), 490 (3.9), 450 (3.8), 319 (4.6); *m/z* (HR-LSIMS) 1242.105010 (M^+). $C_{56}H_{12}B_2F_{16}N_{12}O_4$ requires 1242.103510.

Method b: BCl_3 1 M solution in *p*-xylene (5.5 mL, 5.5 mmol), tetrafluorophthalonitrile (1 g, 5 mmol), and 1,2,4,5-benzenetetracarbonitrile (90 mg, 0.55 mmol).

The crude obtained (consisting of residual SubPc **4** and dimers **2a** and **2b**) was subjected to column chromatography on silica gel using dichloromethane/hexane (3:2, v/v), isolating a mixture of compounds **2a** and **2b** (115 mg, 20%). This fraction was then reacted with 130 mg (1.07 mmol) of 3-hydroxybenzaldehyde, and heated the mixture to 110 °C for 2 h. After cooling, the crude was washed with methanol/water 1:1 and filtered. Compound **3a** was isolated through column chromatography on silica gel with hexane/dichloromethane/acetone 4:2:1, as a reddish blue powder (35 mg, 5% relative to 1,2,4,5-benzenetetracarbonitrile).

Method c: BCl_3 1 M solution in *p*-xylene (5.5 mL, 5.5 mmol), tetrafluorophthalonitrile (1 g, 5 mmol), and 1,2,4,5-benzenetetracarbonitrile (90 mg, 0.55 mmol).

Each precursor (dimers **2a** and **2b**) was isolated as described above (**2a**: 61 mg, 10%; **2b**: 48 mg, 8%) and reacted separately with 3-hydroxybenzaldehyde—69 mg (0.57 mmol) and 55 mg (0.45 mmol), respectively. Following similar work-up as described above, compound **3a** was isolated as a reddish blue powder (33 mg, 47%, 5% global yield). Reaction with dimer **2b** gave only decomposition products.

4.1.4. *syn*-[(C_{60})(Hexadecafluoro)]-subphthalocyanine fused dimer 1. A dry toluene solution (40 mL) of 45 mg (0.04 mmol) of SubPc dimer **3a**, 52 mg (0.07 mmol) of C_{60} fullerene, and 20 mg (0.22 mmol) of sarcosine (*N*-methylglycine) was heated to reflux under argon atmosphere for 18 h. The solution was cooled down to room temperature and the solvent evaporated in vacuo. After column chromatography on silica gel using toluene as eluent, compound **1** was isolated (12 mg, 16%) as a dark blue solid (Found: C, 69.93; H, 1.42; N, 10.04. $C_{120}H_{22}B_2F_{16}N_{14}O_2$ requires: C, 71.45; H, 1.10; N, 9.72%.); ν_{max} (KBr)/cm^{-1} 2923, 2852, 1735, 1635, 1533, 1480, 1384, 1262, 1213, 1168, 1098, 964, 804; δ_H (300 MHz; $CDCl_3$; Me_4Si) 10.20–9.40 (2H, m), 6.4–5.6 (2H, m), 5.50–3.50 (6H, m), 2.80–2.10 (6H, m); δ_F (470 MHz; $CDCl_3$; $CFCl_3$) −137.6 (8F, m), −148.7 (8F, m); λ_{max} ($CHCl_3$)/nm 694 (log ε 5.0), 659 (4.6), 634 (4.6), 606 (4.7), 590 (sh), 491 (4.2), 310 (4.9), 269 (5.1); *m/z* (HR-LSIMS) 2016.194500 (M^+). $C_{120}H_{22}B_2F_{16}N_{14}O_2$ requires 2016.198079.

4.2. Photophysical measurements

Femtosecond transient absorption studies were performed with 580 nm laser pulses (1 kHz, 150 fs pulse width) from an amplified Ti/Sapphire laser system (Model CPA 2101, Clark-MXR Inc.) equipped with a NOPA-Plus. Nanosecond Laser Flash Photolysis experiments were performed with laser pulses from a Quanta-Ray CDR Nd/YAG system (532 nm, 6 ns pulse width) in a front face excitation geometry. Fluorescence lifetimes were measured with a Laser Strobe Fluorescence Lifetime Spectrometer (Photon Technology International) with 337 nm laser pulses from a nitrogen laser fiber-coupled to a lens-based T-formal sample compartment equipped with a stroboscopic detector. Details of the Laser Strobe systems are described on the manufacture's web site, http://www.pti-nj.com. Emission spectra were recorded with a SLM 8100 Spectrofluorometer. The experiments were performed at room temperature. Each spectrum represents an average of at least five individual scans, and appropriate corrections were applied whenever necessary. Pulse radiolysis experiments were performed by utilizing 50 ns pulses of 8 MeV electrons from a Model TB-8/16-1S Electron Linear Accelerator. Details on such equipment, in general, and the data analysis have been described elsewhere.[19,16]

4.3. Electrochemical measurements

Electrochemical measurements were performed on an Autolab PGStat 30 equipment using a three electrodes configuration system. The measurements were carried out using THF solutions containing 0.1 M tetrabutylammonium hexafluorophosphate ($TBAPF_6$). A glassy carbon electrode (3 mm diameter) was used as the working electrode, and a platinum wire and an $Ag/AgNO_3$ in CH_3CN electrode were employed as the counter and the reference electrode, respectively. Ferrocene (Fc) was added as an internal reference and all the potentials were referenced relative to the Fc/Fc^+ couple. Both the counter and the reference electrodes were directly

immersed in the electrolyte solution. The surface of the working electrode was polished with commercial alumina prior to use. Solutions were stirred and deaerated by bubbling argon for a few minutes prior to each voltammetric measurement. Unless otherwise specify the scan rate was 100 mV/s.

Acknowledgements

Funding from the MEC of Spain (CTQ2005-08933/BQU, CTQ2005-02609/BQU, MAT2004-03849, ESF-MEC (project SOHYD), and CONSOLIDER-INGENIO 2010C-07-25200), the Comunidad Autónoma de Madrid (project P-PPQ-000225-0505), and EU (MRTN-CT-2006-035533, Solar-N-type and COST Action D35) is gratefully acknowledged. The electrochemical measurements were performed in the laboratory of Prof. Nazario Martín at the Department of Organic Chemistry at Universidad Complutense, to whom we are very grateful. R.S.I. and M.A.H. would like to thank CAPES of Brazil for a Ph. D. grant and the CICYT for a 'Ramón y Cajal' contract, respectively. We also thank to the Deutsche Forschungs-gemeinschaft (SFB 583), FCI and the Office of Basic Energy Sciences of the U.S. Department of Energy.

References and notes

1. (a) Martín, N.; Sánchez, L.; Illescas, B.; Pérez, I. *Chem. Rev.* **1998**, *98*, 2527–2548; (b) Segura, J. L.; Martín, N.; Guldi, D. M. *Chem. Soc. Rev.* **2005**, *34*, 31–47; (c) *Tetrahedron* **2006**, *62*, 1905–2132, special issue on the supramolecular chemistry of fullerenes.
2. Echegoyen, L. E.; Herranz, M. A.; Echegoyen, L. *Encyclopedia of Electrochemistry*; Bard, A. J., Stratmann, M., Scholz, F., Pickett, C. J., Eds.; Wiley-VCH: Weinheim, 2006; Vol. 7, pp 145–201.
3. (a) Imahori, H.; Sakata, Y. *Adv. Mater.* **1997**, *9*, 537–546; (b) Roncali, J. *Chem. Soc. Rev.* **2005**, *34*, 483–495; (c) Liddell, P. A.; Kodis, G.; Andreasson, J.; De la Garza, L.; Bandyopadhyay, S.; Mitchell, R. H.; Moore, T. A.; Moore, A. L.; Gust, D. *J. Am. Chem. Soc.* **2004**, *126*, 4803–4811; (d) Liu, Y.; Liang, P.; Chen, Y.; Zhao, Y.-L.; Ding, F.; Yu, A. *J. Phys. Chem. B* **2005**, *109*, 23739–23744; (e) Guldi, D. M.; Rahman, G. M. A.; Ehli, C.; Sgobba, V. *Chem. Soc. Rev.* **2006**, *35*, 471–487.
4. (a) De la Torre, G.; Claessens, C. G.; Torres, T. *Chem. Commun.* **2007**, 2000–2015; (b) Guldi, D. M. *Chem. Soc. Rev.* **2002**, *31*, 22–36; (c) Guldi, D. M.; Gouloumis, A.; Vázquez, P.; Torres, T.; Georgakilas, V.; Prato, M. *J. Am. Chem. Soc.* **2005**, *127*, 5811–5813.
5. (a) Claessens, C. G.; González-Rodríguez, D.; Torres, T. *Chem. Rev.* **2002**, *102*, 835–853; (b) Torres, T. *Angew. Chem., Int. Ed.* **2006**, *45*, 2834–2837; (c) Sastre, A.; Torres, T.; Díaz-García, M. A.; Agulló-López, F.; Dhenaut, C.; Brasselet, S.; Ledoux, I.; Zyss, J. *J. Am. Chem. Soc.* **1996**, *118*, 2746–2747; (d) del Rey, B.; Keller, U.; Torres, T.; Rojo, G.; Agulló-López, F.; Nonell, S.; Marti, C.; Brasselet, S.; Ledoux, I.; Zyss, J. *J. Am. Chem. Soc.* **1998**, *120*, 12808–12817; (e) Claessens, C. G.; Gonzalez-Rodriguez, D.; Torres, T.; Martin, G.; Agulló-Lopez, F.; Ledoux, I.; Zyss, J.; Ferro, V. R.; García de la Vega, J. M. *J. Phys. Chem. B* **2005**, *109*, 3800–3806.
6. (a) González-Rodríguez, D.; Torres, T.; Guldi, D. M.; Rivera, J.; Echegoyen, L. *Org. Lett.* **2002**, *4*, 335–338; (b) González-Rodríguez, D.; Torres, T.; Guldi, D. M.; Rivera, J.; Herranz, M. A.; Echegoyen, L. *J. Am. Chem. Soc.* **2004**, *126*, 6301–6313; (c) González-Rodríguez, D.; Claessens, C. G.; Torres, T.; Liu, S.-G.; Echegoyen, L.; Vilá, N.; Nonell, S. *Chem.—Eur. J.* **2005**, *11*, 3881–3893.
7. Claessens, C. G.; González-Rodríguez, D.; Iglesias, R. S.; Torres, T. *C.R. Chim.* **2006**, *9*, 1094–1099.
8. (a) Claessens, C. G.; Torres, T. *Chem. Commun.* **2004**, 1298–1299; (b) Claessens, C. G.; Torres, T. *J. Am. Chem. Soc.* **2002**, *124*, 14522–14523.
9. Claessens, C. G.; González-Rodríguez, D.; del Rey, B.; Torres, T.; Mark, G.; Schuchmann, H.-P.; von Sonntag, C.; MacDonald, J. G.; Nohr, R. S. *Eur. J. Org. Chem.* **2003**, 2547–2551.
10. (a) Claessens, C. G.; Torres, T. *Angew. Chem., Int. Ed.* **2002**, *41*, 2561–2565; (b) Fukuda, T.; Store, J. R.; Potucek, R. J.; Olmstead, M. M.; Noll, B. C.; Kobayashi, N.; Durfee, W. S. *Angew. Chem., Int. Ed.* **2002**, *41*, 2565–2567; (c) Iglesias, R. S.; Claessens, C. G.; Torres, T.; Herranz, M. A.; Ferro, V. R.; García de la Vega, J. M. *J. Org. Chem.* **2007**, *72*, 2967–2977.
11. Iglesias, R. S.; Claessens, C. G.; Torres, T.; Rahman, G. M. A.; Guldi, D. *Chem. Commun.* **2005**, 2113–2115.
12. (a) Nakamura, Y.; Okawa, K.; Matsumoto, M.; Nishimura, J. *Tetrahedron* **2000**, *56*, 5429–5434; (b) Kordatos, K.; Bosi, S.; Da Ros, T.; Zambon, A.; Lucchini, V.; Prato, M. *J. Org. Chem.* **2001**, *66*, 2802–2808.
13. Boudon, C.; Gisselbrecht, J.-P.; Gross, M.; Isaacs, L.; Anderson, H. L.; Faust, R.; Diederich, F. *Helv. Chim. Acta* **1995**, *78*, 1334–1344.
14. (a) Kessinger, R.; Gómez-López, M.; Boudon, C.; Gisselbrecht, J.-P.; Gross, M.; Echegoyen, L.; Diederich, F. *J. Am. Chem. Soc.* **1998**, *120*, 8545–8546; (b) Carano, M.; Da Ros, T.; Fonti, M.; Kordatos, K.; Marcaccio, M.; Paolucci, F.; Prato, M.; Bofia, S.; Zerbetto, F. *J. Am. Chem. Soc.* **2003**, *125*, 7139–7144; (c) Li, K.; Schuster, D. I.; Guldi, D. M.; Herranz, M. A.; Echegoyen, L. E. *J. Am. Chem. Soc.* **2004**, *126*, 3388–3389.
15. These calculations do not intend to reproduce the outcome of the kinetically controlled Prato reaction but rather the relative thermodynamic stability of the possible isomers.
16. Schick, G.; Hirsch, A.; Mauser, H.; Clark, T. *Chem.—Eur. J.* **1996**, *2*, 935–943.
17. The shortest distance between a carbon atom from C_{60} and one from the dimer central ring.
18. This equilibrium distance is larger than the optimal distance between two π–π interacting rings (3.4 Å) as a consequence of the steric hindrance brought by the two pyrrolidine moieties.
19. Hug, G. L.; Wang, Y.; Schöneich, C.; Jiang, P.-Y.; Fessenden, R. W. *Radiat. Phys. Chem.* **1999**, *54*, 559–566.